

## Nonequilibrium phase transitions in a driven sandpile model

This article has been downloaded from IOPscience. Please scroll down to see the full text article.

1995 J. Phys. A: Math. Gen. 28 L563

(<http://iopscience.iop.org/0305-4470/28/22/001>)

View [the table of contents for this issue](#), or go to the [journal homepage](#) for more

Download details:

IP Address: 171.66.16.68

The article was downloaded on 02/06/2010 at 00:55

Please note that [terms and conditions apply](#).

## LETTER TO THE EDITOR

# Non-equilibrium phase transitions in a driven sandpile model

Sujan K Dhar†, Rahul Pandit†§ and Sriram Ramaswamy††§

† Department of Physics, Indian Institute of Science, Bangalore 560 012, India

‡ Centre for Theoretical Studies, Indian Institute of Science, Bangalore 560 012, India

Received 30 May 1995

**Abstract.** We construct a driven sandpile slope model and study it by numerical simulations in one dimension. The model is specified by a threshold slope  $\sigma_c$ , a parameter  $\alpha$ , governing the local current-slope relation (beyond threshold), and  $j_{in}$ , the mean input current of sand. A non-equilibrium phase diagram is obtained in the  $\alpha$ - $j_{in}$  plane. We find an infinity of phases, characterized by different mean slopes and separated by continuous or first-order boundaries, some of which we obtain analytically. Extensions to two dimensions are discussed.

The statistical mechanics of non-equilibrium steady states is a subject of growing general interest. Phase transitions between such states are by no means as well understood as their equilibrium counterparts. Some insight has been gained into this problem by the study of simple driven lattice models [1, 2]. Sandpile models, which introduced the notion of *self-organized criticality* (SOC) [3] as a general explanation for the wide occurrence of power laws in nature, are a natural setting in which to study phase transitions far from equilibrium. Surprisingly, to our knowledge, this has not been attempted. We construct a driven sandpile model and show that it exhibits, in spite of its simplicity, a rich phase diagram, thus making it a good laboratory for the study of non-equilibrium phenomena. In particular, our model exhibits continuous transitions from pinned or threshold-dominated states to unpinned states; these are reminiscent of dynamical phase transitions in more complex systems such as sliding charge-density waves (CDWs) [4] and pinned flux lattices [5].

Earlier studies of sandpile models have concentrated on SOC, either in steadily flowing sandpiles [6, 7] or at the angle of repose [8]. Much of the work has been on *critical-height* models, in which the update rule depends only on the *height* at each site; *critical-slope* models (CSM) [8] have been studied to a lesser extent. In this letter, we present a comprehensive study of a simple CSM in which the current-slope relation for slopes exceeding a threshold is controlled by a parameter  $\alpha$ . We monitor the steady states of our model as a function of  $\alpha$  and the mean input current  $j_{in}$  and find a rich non-equilibrium phase diagram (figure 1): it shows that there are many phases characterized by the average slope  $\sigma_{av}$  of the sandpile. In the pinned repose phase,  $\sigma_{av} = \sigma_c$ , the slope at the angle of repose (we use the word *pinned* in the sense that the slope of the sandpile is fixed at the nominal angle of repose for a range of values of the mean input current  $j_{in}$ ). As  $j_{in}$  is increased at fixed  $\alpha$ , the repose phase undergoes a continuous transition (full curve) to

§ Also at: Jawaharlal Nehru Centre for Advanced Scientific Research, Bangalore, India.

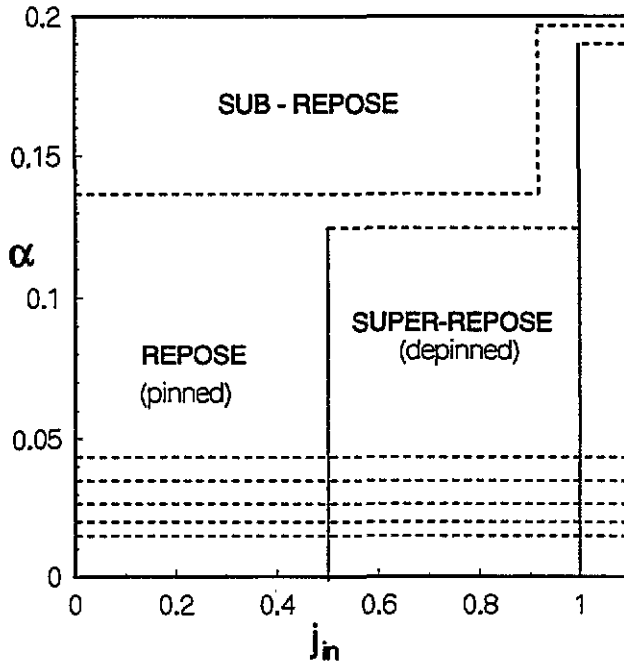


Figure 1. The non-equilibrium phase diagram of our model in the  $\alpha$ - $j_{in}$  plane. Full (broken) lines indicate continuous (first-order) transitions. At low  $\alpha$  there is an infinity of first-order boundaries; only the first five are shown. The corners in the phase boundaries and multicritical points are schematic; our data are too noisy to resolve them.

an unpinned super-repose phase at which  $\sigma_{av} - \sigma_c$  rises continuously from zero with an exponent  $\beta \simeq 0.5$  (figure 2). This continuous transition is followed by a series (which we argue is infinite) of similar continuous transitions. The repose phase lies between two first-order boundaries: one at low  $\alpha$  to a pinned super-repose ( $\sigma_{av} > \sigma_c$ ) region, the other at large  $\alpha$ , to a sub-repose phase ( $\sigma_{av} < \sigma_c$ ). The lower one of these first-order lines meets the continuous line at  $j_{in} = 0.5$  at a multicritical point. The pinned super-repose region contains an infinity of phases, separated by first-order lines parallel to the  $j_{in}$  axis (figure 1);  $\sigma_{av}$  jumps at these boundaries. We also monitor height profiles, the equal-time height correlation function, the associated correlation length, current autocorrelations and the associated correlation time. Both the correlation length and time (figure 3) diverge at the continuous transitions in figure 1. We show that our main results can be understood on the basis of a mean-field theory and a mode-softening argument.

In our model, integers  $h_i$  specify the heights of columns of sand at the sites  $i$  of a one-dimensional chain ( $1 \leq i \leq N$ ). The stability of the column at a site is determined by a threshold condition which mimics the angle of repose for a real sandpile: when the height difference between a site  $i$  and its right neighbour ( $i + 1$ ) (i.e. the local slope  $\sigma_i = h_i - h_{i+1}$ ) exceeds  $\sigma_c$ , some sand topples to the right neighbour, and  $h_i$  is updated via

$$h_i \rightarrow h_i - j_i \quad h_{i+1} \rightarrow h_{i+1} + j_i \quad (1)$$

$$j_i = \mathcal{N}(\alpha \times \sigma_i) \ominus (\sigma_i - \sigma_c) \quad (2)$$

where  $\mathcal{N}(x)$  is the integer nearest to  $x$ ,  $\ominus$  is the step function, and  $\alpha$  a real number. This part of our update rule conserves the number of particles locally and yields a local current

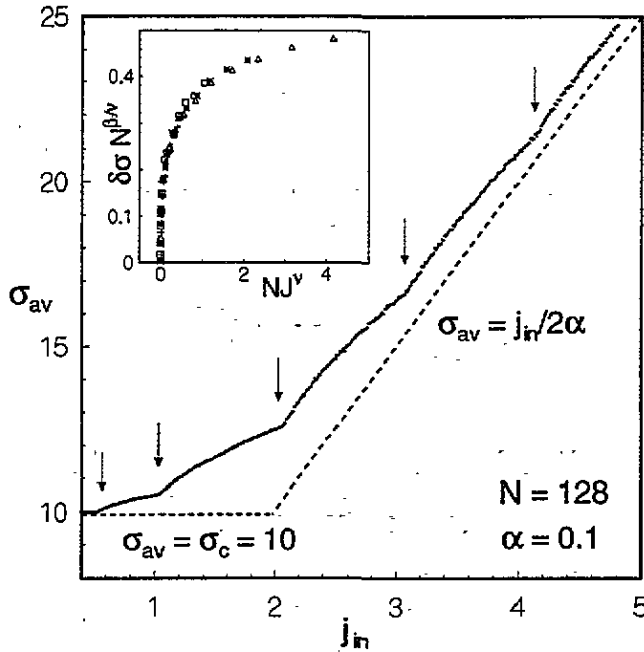


**Figure 2.** A plot (full curve) of  $\sigma_{av}$  versus  $j_{in}$ . Broken lines are the asymptotes for large and small  $j_{in}$ . Arrows mark successive onsets (see the text). The inset shows a finite-size scaling plot for  $\delta\sigma N^{\beta/\nu}$  versus  $NJ^\nu$  at  $\alpha = 0.1$  and  $j_{in} \gtrsim 0.5$  for  $N = 64$  (+),  $128$  (o),  $256$  (\*) and  $512$  ( $\Delta$ ) with  $\beta = 0.5$  and  $\nu = 4$ .

which increases with the local slope, thus preventing an unbounded buildup of particles in the pile $\dagger$ . The parameter  $\alpha$  controls the current-slope relation for slopes exceeding  $\sigma_c$ . We restrict our study to  $\alpha > 0$ , since  $\alpha \leq 0$  yields unphysical runaway behaviour; the upper bound for  $\alpha$  is chosen to limit the region we explore. The mean input current of sand particles  $j_{in}$  is another control parameter. At each time step, we add  $m$  particles to a randomly chosen site with probability  $p$ , so  $j_{in} = p \times m$ . We set  $m = 10$  for specificity (our results do not depend on this choice) and cover the range  $0.001 \leq p \leq 0.15$ , so  $0.01 \leq j_{in} \leq 1.5$ . This addition of particles violates local particle conservation; and, for such an addition rate, the mean input current and the noise amplitude *per site* vanish as  $N \rightarrow \infty$ . Particles are allowed to leave our system through the right, but not the left ( $i = 1$ ), boundary: any particle that reaches the  $N^{\text{th}}$  site is removed immediately. Our boundary conditions and update rules (1, 2) clearly pick a direction for the current (from left to right).

We use initial conditions in which  $h_i = \sigma_c(N - i) + \delta_i$ , where  $\delta_i$  is an integer that assumes the values  $0, \pm 1$  with equal probability. We update all sites simultaneously and allow the system to evolve until it attains a steady state, i.e. when  $j_{in} = j_{out}$ , the average output current (the average number of particles dropping out from the open boundary per unit time). In practice, we say that the steady state has been achieved when these two

$\dagger$  We have also studied a single-step model in which only one particle is transferred when  $\sigma_i > \sigma_c$ . This model displays the first of the onsets of figure 2 with the same exponents; however, the heights become unbounded for  $j_{in} > 1$ . A similar model studied in [7] by Carlson *et al* showed no continuous transitions since the high-noise limit was studied. Further, if we use real continuous heights  $h_i$ , with  $\Theta(\sigma_i - \sigma_c) \rightarrow \frac{1}{2}[1 + \tanh((\sigma_i - \sigma_c)/\gamma)]$ , the onset is replaced by a smooth crossover which becomes a sharp transition as  $\gamma \rightarrow 0$ .

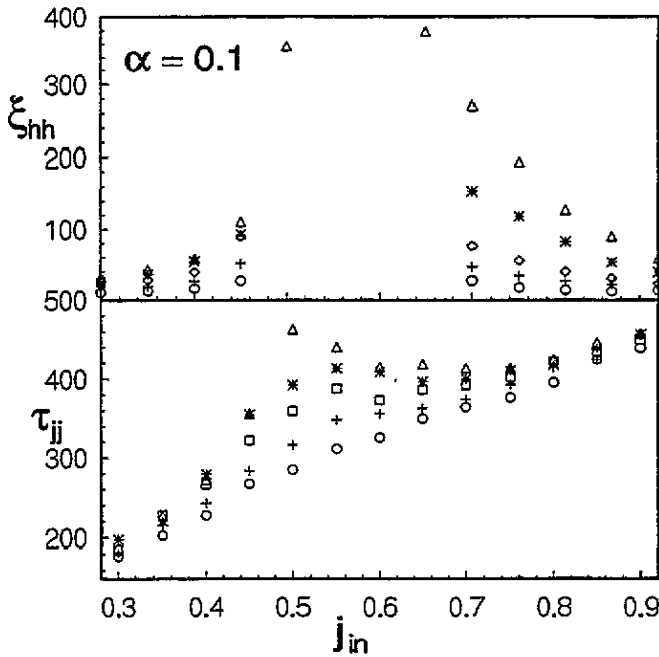


Figure 3. Equal-time height correlation length  $\xi_{hh}$  and output current autocorrelation time  $\tau_{jj}$  versus  $j_{in}$  for  $N = 32$  ( $\circ$ ),  $64$  ( $+$ ),  $128$  ( $\diamond$ ),  $256$  ( $*$ ) and  $512$  ( $\Delta$ ). For  $\xi_{hh}$  we do not plot points in regions where  $\xi_{hh} > N$ .

currents are within 1% of each other. Once the steady state is obtained<sup>†</sup>, we accumulate data for  $10^5$ – $10^6$  updates per site (UPS). Data for averages are stored after every 50 UPS. We also average our data over 10–50 different initial conditions. To minimize boundary effects we ignore a few sites (three or more if necessary) near each boundary while computing all averages.

The non-equilibrium steady state of our model can be characterized by the mean slope  $\sigma_{av}$  (the local slope  $\sigma_i$  averaged over  $i$  and many time steps), which is the order parameter for our model. We also monitor the mean current  $j_{av}$ , the output current  $j_{out}$ , the equal-time height correlation function  $C_{hh}(r) = \langle \langle [h_i^t - \langle h_i \rangle_t][h_{i+r}^t - \langle h_{i+r} \rangle_t] \rangle \rangle_t$ , and the output current autocorrelation function  $C_{jj}(\tau) = \langle [j_{out}^t - \langle j_{out} \rangle_t][j_{out}^{t+\tau} - \langle j_{out} \rangle_t] \rangle_t$ , where  $\langle \dots \rangle_i$  and  $\langle \dots \rangle_t$  denote averages over  $i$  and time  $t$  respectively.

In figure 2 the asymptotes (broken lines)  $\sigma_{av} = \sigma_c$  and  $\sigma_{av} = j_{in}/(2\alpha)$  indicate the behaviour of  $\sigma_{av}$  at very low ( $< 0.5$ ) and very large ( $\gg 0.5$ )  $j_{in}$ , respectively. The full curve (for  $\alpha = 0.1$  and  $N = 128$  in figure 2) shows that the approach to these limits is non-trivial: as  $j_{in}$  increases there are successive onsets, indicated by arrows. There might well be an infinity of such onsets (see below), but they become hard to resolve numerically at large  $j_{in}$ . The inset shows a finite-size scaling plot at the first of these onsets. For  $j_{in} \lesssim 0.5$ ,  $\sigma_{av} = \sigma_c = 10$ , i.e. we have threshold-dominated behaviour at low  $j_{in}$ . The asymptotic behaviours can be understood via the mean-field theory presented below.

<sup>†</sup> The time required to reach the steady state increases as  $N^2$ ; also it is high for  $\alpha \simeq 0$  and  $\alpha \simeq 0.5$  and seems to increase monotonically with decreasing  $j_{in}$ .

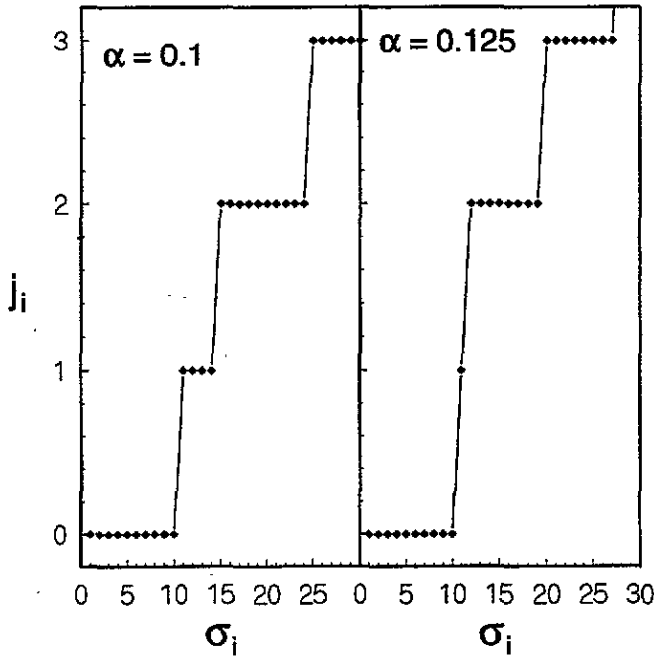


Figure 4. A plot of  $j_i$  versus  $\sigma_i$  (equation (2)) for  $\alpha = 0.1$  and  $0.125$  and  $\sigma_c = 10$ .

The evolution equation for  $h_i^t$  is

$$h_i^{t+1} - h_i^t = -j_i^t + j_{i-1}^t + \eta_i^t \tag{3}$$

where the noise  $\eta_i^t$  has a mean  $j_{in}/N$  that accounts for the addition of particles. If we average over this noise, then, in the steady state, we get  $j_i - j_{i-1} = j_{in}/N$ . If we impose the boundary condition  $j_{i=N} = j_{in}$ , we get  $j_i = i j_{in}/N$  and thence a mean current  $j_{av} = \langle \langle j_i \rangle_t \rangle = \frac{N+1}{2N} j_{in} \approx j_{in}/2$  for  $N \rightarrow \infty$ . We use these exact results to check our simulation. Our mean-field theory assumes that

$$\langle \langle \mathcal{N}(\alpha \sigma_i) \Theta(\sigma_i - \sigma_c) \rangle_{i,t} \rangle \simeq \langle \langle \mathcal{N}(\alpha \sigma_i) \rangle_{i,t} \rangle \langle \langle \Theta(\sigma_i - \sigma_c) \rangle_{i,t} \rangle. \tag{4}$$

For large  $j_{in}$ , most  $\sigma_i > \sigma_c$ , so we further assume  $\langle \langle \Theta(\sigma_i - \sigma_c) \rangle_{i,t} \rangle \simeq 1$ . If its argument is large, the discontinuities of  $\mathcal{N}(\alpha \sigma_i)$  are small relative to  $\alpha \sigma_i$ , so, on averaging (2), we make the approximation  $j_{av} = \langle \langle \mathcal{N}(\alpha \sigma_i) \rangle_{i,t} \rangle = \alpha \sigma_{av}$ ; whence  $\sigma_{av} \approx j_{in}/(2\alpha)$ , the large- $j_{in}$  asymptote of figure 2. Given these approximations, equation (3) yields a discrete diffusion equation for  $h_i^t$  with a spatially uniform source  $j_{in}/N$ . If we solve this with our boundary conditions we get parabolic height profiles for large  $j_{in}$ , which we also find in our simulations [9].

The current-slope relation (2), shows that (figure 4) for a uniform profile with slope  $\sigma$ , no current flows if  $\sigma \leq \sigma_c$ . For  $\sigma > \sigma_c$ , the current grows with the slope in discrete steps, which reflect the  $\mathcal{N}$  function in (2). As we increase  $\alpha$ , the width of the step at  $j_i = 1$  shrinks until it becomes a single point at  $\alpha = 0.125$ , the value at which the continuous transition at  $j_{in} = 0.5$  (figure 1) terminates. This can be understood as follows: if we turn figure 4 on its side, we see that the slope is pinned at  $\sigma_c$  below some threshold value of  $j_i$ . Beyond this threshold, the slope rises sharply before it saturates at another value of  $\sigma$ . The onsets in figure 2 are just the sharp steps of figure 4 rounded by our spatiotemporal average.

The vanishing of a step in figure 4 can also be linked with the termination of the continuous line via a mode-softening argument. Consider, for example, the step at  $j_i = 1$

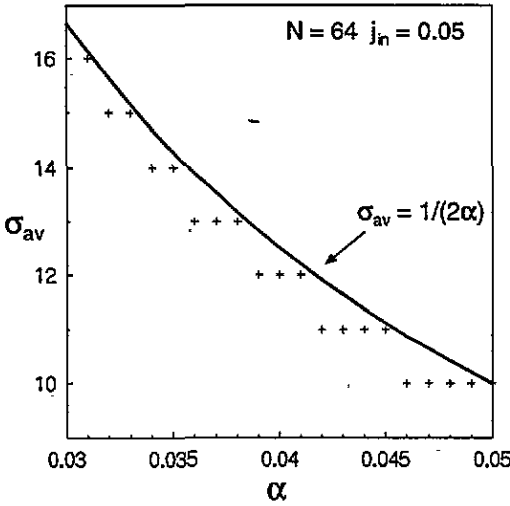


Figure 5. Variation of  $\sigma_{av}$  with  $\alpha$  for  $N = 64$  and  $j_{in} = 0.05$ . The first-order jumps in  $\sigma_{av}$  can be clearly seen from this figure. The overall envelope of the steps fits to the form  $\sigma_{av} = 1/(2\alpha)$  (see the text).

for which the  $11 \leq \sigma_i \leq 14$  (figure 4 with  $\alpha = 0.1$ ). All slopes  $\sigma_i$  in this interval are equivalent in the sense that the sandpile dispenses the same amount of local current for all of them. Thus the restoring force, in response to a change of an on-site slope from  $\sigma$  to  $\sigma + 1$ , vanishes and leads to divergent correlation lengths and relaxation times (figure 3). Clearly the infinity of steps in figure 4 imply an infinity of onsets in figure 2, though the large- $j_{in}$  onsets are hard to resolve numerically.

The above arguments do not yield the value of  $j_{in}$  at onset since our spatiotemporal average shifts the values of the thresholds in figure 4. The actual value of  $j_{in}$  at the onset depends on the distribution of slopes in the interior of the pile. We have done some numerical and analytic calculations [9] on a 'single-step model' (see footnote on page L565), which justify the occurrence of the transition at  $j_{in} = 0.5$ .

For the first onset we calculate the mean slope near  $j_{in} \simeq 0.5$  for  $\alpha = 0.1$  and  $N = 32, 64, 128, 256$  and  $512$  and from a finite-size-scaling analysis (figure 2) obtain the exponents  $\beta = 0.5$  and  $\nu = 4.0$ , where  $J \equiv |j_{in} - j_c|/j_c$  with  $j_c = 0.5$ , and we use the scaling form  $\delta\sigma = N^{-\beta/\nu} \mathcal{F}(J^\nu N)$ , with  $\delta\sigma \equiv \sigma_{av} - \sigma_c$ . The exponent  $\nu$ , which we obtain in this way from finite-size scaling, might not be the same as the actual correlation length exponent as has been pointed out in the context of sliding CDWs [4].

In the low- $j_{in}$  regime, as  $\alpha$  increases from 0 to 0.05,  $\sigma_{av}$  decreases in steps of one (figure 5). The values of  $\alpha$  at which these steps occur yield the first-order boundaries of figure 1. All these first-order boundaries end at critical points in the range  $1 \lesssim j_{in} \lesssim 1.2$ . The overall envelope of the steps in  $\sigma_{av}$  can be fit approximately to a form  $\sigma_{av} \sim 1/(2\alpha)$ . This behaviour follows from the update rule equation (2):  $\mathcal{N}(\alpha\sigma_i) = 0$  for  $\alpha\sigma_i < \frac{1}{2}$ , so, if  $\alpha < 1/(2\sigma_c)$  ( $= 0.05$  for  $\sigma_c = 10$ ), even a slope  $\sigma_i > \sigma_c$  may become stable; e.g. with  $\sigma_c = 10$  and  $\alpha = 0.04$ ,  $\mathcal{N}(\alpha\sigma_i) = 0$  for  $\sigma_i = \sigma_c + 1$  and  $\sigma_c + 2$ , so the slope at the effective angle of repose turns out to be  $\sigma_{eff} = \sigma_c + 2 = 12$ . As  $\alpha$  decreases,  $\sigma_{eff}$  also increases in discrete steps, leading to the first-order lines at low  $\alpha$ .

We fit the equal-time height correlation function  $C_{hh}(r)$  to an exponential form [9] which then yields a correlation length. Figure 3 shows this correlation length  $\xi_{hh}$  versus  $j_{in}$  for  $\alpha = 0.1$  at different values of  $N$ . Clearly  $\xi_{hh}$  diverges at  $j_{in} \simeq 0.5$  and also at subsequent continuous transitions. We have not characterized the divergences by an exponent because  $\xi_{hh}$  exceeds our system size somewhat before the transition (so we do not show data near  $j_{in} = 0.5$ ).

The output current autocorrelation function  $C_{jj}(\tau)$  does not fit an exponential form very well. However, we have extracted correlation times  $\tau_{jj}$  from the area under  $C_{jj}(\tau)$  (normalized so that  $C_{jj}(\tau = 0) = 1$ ). Figure 3 shows plots of  $\tau_{jj}$  versus  $j_{in}$  for  $\alpha = 0.1$ , which sharpen with increasing  $N$ . This sharpening shows up clearly near  $j_{in} = 0.5$  and leads to an increasing trend in  $\tau_{jj}$  near the next onset ( $j_{in} \simeq 1.1$ ).

It is generally believed that non-equilibrium phase transitions cannot occur in stochastic, one-dimensional models with short-range interactions [10], though there are a few recent counterexamples [11]. Our model provides yet another counterexample. We believe the transitions in our model occur because the noise amplitude per site vanishes as  $N \rightarrow \infty$ . This is why our one-dimensional model with short-range interactions exhibits phase transitions. We have checked that these phase transitions get rounded if there is a finite noise amplitude per site as  $N \rightarrow \infty$ . We have also performed simulations on two-dimensional versions of our model. Our preliminary results indicate that, with low noise and a variety of boundary conditions, such two-dimensional models show the same transitions as the one-dimensional model discussed here. In the steady state, the two-dimensional system behaves like an uncoupled one-dimensional system, so no transitions occur in the high-noise limit. The details of this study will be published elsewhere [9].

We have shown that our driven sandpile model displays a variety of steady states and many transitions between them. This richness, coupled with its simplicity, makes our model a promising one for the study of non-equilibrium phenomena in driven systems. As noted above, it displays transitions similar to those in other driven systems, e.g. our onset transitions (figure 2) are like unpinning transitions in sliding CDWs [4] or in pinned flux-lattice systems [5] although clearly in a different universality class. It would be interesting to study whether this similarity is merely superficial. There are some obvious ways in which the CDW models are different from ours: (i) they exhibit pinning because of quenched randomness but have no external noise; and (ii) no current flows in their pinned states. The importance of these differences needs to be elucidated. In this general context it is interesting to study the zero-current limit of our model. We find that it *does not* show conventional SOC when the pile is allowed to relax, after each input of sand, to a completely quiescent state in which no further transfers are possible (à la Bak *et al* [3]). The precise forms of the distribution of avalanche sizes, etc, will be reported elsewhere [9].

We thank CSIR and BRNS (India) for support, and the SERC (IISc Bangalore) for computational facilities.

## References

- [1] Schmittmann B and Zia R K P 1995 Statistical mechanics of driven diffusive systems *Phase Transitions and Critical Phenomena* ed C Domb and J Lebowitz (London: Academic) to appear
- [2] He Y, Jayaprakash C and Grinstein G 1990 *Phys. Rev. A* **42** 3348
- [3] Bak P, Tang C and Wiesenfeld K 1987 *Phys. Rev. Lett.* **59** 381; 1988 *Phys. Rev. A* **38** 364
- [4] Narayan O and Fisher D S 1992 *Phys. Rev. B* **46** 11 520
- [5] Bhattacharya S and Higgins M J 1993 *Phys. Rev. Lett.* **70** 2617  
Pla O and Nori F 1991 *Phys. Rev. Lett.* **67** 919
- [6] Hwa T and Kardar M 1989 *Phys. Rev. Lett.* **62** 1813; 1992 *Phys. Rev. A* **45** 7002
- [7] Carlson J M, Grannan E R and Swindle G H 1993 *Phys. Rev. E* **47** 93
- [8] Kadanoff L P, Nagel S R, Wu L and Zhou S M 1989 *Phys. Rev. A* **39** 6524
- [9] Dhar S K, Pandit R and Ramaswamy S to be published
- [10] Liggett T M 1985 *Interacting Particle Systems* (New York: Springer) p 201
- [11] Evans M R, Foster D P, Godrèche C and Mukamel D 1995 *Phys. Rev. Lett.* **74** 208